Experimental Studies of Active Temperature Control in Solid Breeder Blankets

M. S. Tillack, A. R. Raffray, A. Y. Ying, M. A. Abdou, and P. Huemer
Mechanical, Aerospace and Nuclear Engineering Department
University of California, Los Angeles, CA 90024

Abstract

A program of model development and experimentation has been undertaken to develop innovative methods to provide predictable and controllable thermal barrier regions for solid breeder blankets. In particular, particle beds have been studied because of their unique thermal-hydraulic properties. It has been demonstrated that large variations in thermal conductance can be obtained in the thermal barrier region by external control over the gas pressure and composition in a metallic particle bed. By providing this "active" control mechanism, adjustments in the blanket temperature profiles can be made **during operation** to accommodate changes in power levels, time-dependent changes in material behavior, and design uncertainties.[1] Data are presented for the effective thermal conductivity of several single-size and binary beds of aluminum, for a range of He and N_2 gas pressures, and for a number of different porosities. Data for the wall conductance also are presented. The relative contribution to the temperature drop due to wall conductance is smallest in single-size beds with smaller particles. The variation of wall conductance with pressure is small or non-existent, suggesting that the wall region is dominated by conduction through the solid particle contact points, rather than gas in the Smolukovski zones.

1. Introduction

One of the largest remaining uncertainties in the operation of solid breeder blankets is thermomechanical behavior in the fusion environment. Stable and predictable temperature profiles are important for adequate tritium release and to maintain each blanket element within its allowable operating range. The main uncertainties usually arise at interfaces, such as between the breeder and cladding, or between the multiplier and its cladding.

For adequate tritium release from a ceramic breeding blanket, the breeder material is generally kept between about 400 and 1000°C, depending on the breeder material. The coolant temperature is often lower, particularly in experimental fusion devices; for example, in ITER the water coolant is

kept below 100°C. In order to maintain the breeder within its allowable temperature window, most designs utilize a thermal barrier of some type (*e.g.*, a gas gap) between the breeder and coolant.

The ability to actively control (in-situ) the thermal resistance between the breeder, multiplier, and coolant can make solid breeder designs substantially more flexible and attractive for both ITER as well as commercial power reactor applications. Experimental studies are being carried out to explore mechanisms for active thermal control, and to define the limits of usefulness for these schemes.

One such control mechanism uses metallic Be particle beds, as proposed for the ITER ceramic breeder blanket design.[2,3] The packed bed consists of a dispersion of gas and stagnant solid particles. Control of the effective thermal conductivity of the bed is obtained through the Smolukovski effect, whereby changes in the gas pressure and composition can substantially alter the effective thermal conductivity of the bed. This behavior is affected also by the nature of the particle contact and by the size and surface characteristics of the particles.

Experiments were conducted for both single size and binary particle distributions under different gas pressures and flow rates. Aluminum was chosen to simulate the physical properties of beryllium, which is the material proposed for reactor applications. Helium and nitrogen are used for the gas component. Results show that substantial (as high as a factor of 4) changes in thermal conductance can be achieved through active control.

A previous work [4] reported initial results, which were promising. The present work attempts to confirm and expand on these earlier results. A new test section was constructed with enhanced instrumentation and a wider range of operating pressures and temperatures. Both bulk conductivity as well as wall conductances are reported.

2. Description of the experimental apparatus

2.1. Test section and flow loop

The particle bed is contained in an annular region 30.5 cm long with inner and outer diameters of 2.9 cm and 14 cm respectively. A cartridge heater at the center provides the heat source and a water cooling tube running around the outside provides cooling (see Figure 1). The inner and outer cladding and all other metallic parts are made of aluminum. End losses are minimized by

using bakelite end caps. The gas plena at the top and bottom also help to insulate against end losses.

Thermocouples are inserted through Swagelok fittings to provide leak tightness and the ability to remove all instrumentation. Both axial and radial penetrations are provided at two circumferential locations for redundant temperature measurements. The same fittings can be used for pressure gradient measurements. The axially inserted thermocouples are placed at 5 different radial positions to provide enough data to derive the radial temperature gradient. Their spacing is smaller near the inner clad where the gradient is higher.

An aluminum "thermocouple tube" was also provided between the inner clad and heater. Thermocouples were laid in grooves in this tube at various locations. These inner clad temperatures are necessary to evaluate the wall conductance (h). Thermocouples were not provided at the bed outer radius because the temperature gradient is generally too low there to make an accurate determination of h.

The gas flow loop is shown in Figure 2. It was designed to provide the ability to evacuate the test section and back fill with different gas pressures, and to perform flowing gas experiments (which are not reported here). Temperatures and pressures can be measured at various locations, as shown in Fig. 2. An expansion tank improves flow stability and reduces fluctuations. Two pumps provide for different flow regimes: a low-flow tubing pump and a high throughput rotary vane pump.

2.2. Material forms and test matrix

Extensive data have been accumulated for the bulk thermal conductivity in Al beds with He and N_2 gas constituents. Three particle sizes were studied, as described in Table 1. In addition, binary beds were created using all combinations of the three sizes.

All beds were packed and measured several times to establish the reproducibility of the data. Temperature profiles were measured in each bed for gas pressures ranging from ~0.005–3 atm. The packing procedure is very important to obtain uniform tight packing. A vibratory table was used with good success. In binary beds, a two-step procedure was used whereby the large fraction is packed first and then the smaller fraction is allowed to sift through the bed using vibration. The method is described more thoroughly in [4]. Even using this careful procedure, a

variation of several percent in average packing fraction was observed for beds of the same composition.

3. Equations and definitions

Assuming the bed is uniform, axisymmetric and steady state, the experimental value of the effective thermal conductivity is derived from the measurement of temperatures using the equation for the temperature profile in an annulus:

$$k_{eff} = \frac{Q \log(r_o/r_i)}{2\pi L \Delta T} \qquad (1)$$

where
Q = power to the heater
r_o, r_i = inner and outer radii of the bed
L = heated length
ΔT = temperature difference across the bed.

The experimental accuracy of measuring the effective thermal conductivity of a packed bed depends partly on the accuracy with which the relevant temperature difference, the input power, and the geometrical dimensions can be determined. This error can be estimated using the following equation:

$$\frac{\sigma_k}{k_{eff}} = \sqrt{U_Q^2 + U_{ro}^2 + U_{ri}^2 + U_L^2 + U_{Ti}^2 + U_{To}^2} \qquad (2)$$

where $U_i = \frac{\sigma_i}{k_{eff}} \frac{\partial k_{eff}}{\partial x_i}$ represents the contribution to the error in k_{eff} from the various terms in Eq. 1, and σ_i is the error in parameter x_i. Generally, the instrumental error in the measurement of k_{eff} is ~10%.

Additional errors arise due to the lack of circumferential and axial uniformity. However, the actual errors in the measured temperature profiles and heat fluxes near the mid-plane are much less than the global errors in the heat flux. This is due to the fact that the heater is designed to provide constant heat flux through the entire length, and consequently, due to axial symmetry, the radial heat flux near the mid-plane is only slightly affected by axial end losses.

A small temperature difference occurs between the measurement of temperature at the inner wall and the extrapolated temperature from the bed to the wall. This occurs primarily because the

presence of a wall disturbs the local packing, resulting in higher local porosity and additional resistance to heat transfer.

The temperature jump at the inner and outer walls of the bed can be determined by extrapolating the bed internal temperatures to the wall using a linear regression fit of T vs. log(r). The extrapolated temperature is then compared with the measured temperature at the wall. The temperature difference is used to determine an effective wall conductance:

$$q = h\,\Delta T \tag{3}$$

where

q = surface heat flux
ΔT = temperature difference between wall and bed extrapolation
h = the wall conductance

The experimental error in h can be much larger than k_{eff} because the temperature difference ΔT is usually small (several °C) and because the bed internal temperatures must be extrapolated to the wall. A small error in the gradient in the bed can extrapolate to a relatively larger temperature uncertainty at the wall. The error is calculated as above:

$$\frac{\sigma_h}{h} = \sqrt{U_q^2 + U_{Ti}^2 + U_{Te}^2} \tag{4}$$

where T_e is the extrapolated temperature. The error in the extrapolated temperature is obtained from the error in the coefficients of the least squares fit of temperature [5]. For cases in which $\Delta T > 5$°C, the error in h is ~20%. For cases in which $\Delta T < 5$°C, the error can become quite large. The value of q ranges from 3000–6000 W/m^2 (depending on the gas used). From Eqs. 3 and 4, and assuming $U_{\Delta T} \sim 2$°C, the largest h which can be resolved experimentally is of the order of 1500–3000. In other words, if h is larger than ~1500 W/m^2-K, then the resulting temperature jump at the wall is less than the measurement uncertainty.

4. Thermal conductivity data

Results of several redundant tests show good reproducibility of the data – within ±10%. Each time a new bed is packed, a slightly different packing fraction is obtained, which can have a substantial effect on the conductivity at higher pressures. Figures 3–5 show the effective thermal conductivity

in 4.3-mm, 0.5-mm, and 0.1-mm single-size beds. The powder bed shows the largest variation of conductivity with pressure – a factor of four change from 0.1 atm to 3 atm. This is believed to be due to the poorer metal-to-metal contact resulting from surface roughness and irregular shapes, which leads to greater relative influence by the gas phase. A change of packing fraction by .025 changes the high-pressure conductivity by 10–15%.

The more recent data extends to lower pressures. At very low pressure, the He data tends to meet with the N_2 data, indicating that gas conduction is essentially eliminated and heat is transferred through the solid contacts alone below ~0.1 atm.

The data for binary beds indicates a strong variation with packing fraction. There is a smaller percentage variation of thermal conductivity with pressure, as compared with the single-size beds having particle size the same as the smaller particles in the binary bed. The conductivity at 1 atm changes from 6 to 9.5 W/m-K as the packing fraction increases from 80% to 86%. As with single-size beds, the conductivity at low pressure tends to coincide with that of N_2, suggesting that solid contact conductance dominates in this regime. Figure 6 summarizes several data sets with a binary 0.5+4.3 mm bed and He and N_2 fill gas. Figure 7 summarizes data with a binary 0.1+4.3 mm bed and He fill gas only. Porosities are shown next to the curves.

5. Wall conductance data

The temperature gradient increases near the wall for two reasons: the local packing fraction decreases near the wall, and the number of contact points per unit volume decreases (due in part to changes in the packing geometry). The relative effect of the wall region is expected to increase as the particle diameter increases, because the size of the wall region increases with particle size. For 4.3-mm balls, the temperature jump was 10–15°C (with q~3000 W/m^2), which is large enough to measure accurately. However, for single-size beds with 0.5-mm or 0.1-mm particles, the temperature jump at the wall is observed to be a small fraction of the temperature difference across the bed (<5–10%). In these cases, the actual value of the temperature jump is usually less than ~5°C, and the data have large uncertainties. We can only state that in these cases the wall conductance is greater than ~1500 W/m^2-K.

Figure 8 shows data for the wall conductance (h) in a single-size 4.3-mm bed with both He and N_2 fill gas. A small increase in h is seen for He as the pressure increases from 0 to 1 atm (although the uncertainty is a large fraction of the total variation with pressure). The variation is only ~20%, in contrast with k_{eff} which varies by a factor of 3. This suggests that the role of the gas phase is

reduced near the wall, and relatively more conduction occurs through contact points. In support of this conclusion is the N_2 data. With N_2 fill gas, the variation with pressure is absent, and the absolute magnitude is only slightly lower than with He fill gas. This suggests that the contribution to the wall conductance from the gas phase is small even with He.

Another case of interest is the binary beds, in which the bed conductivity is so large that the wall region can cause a significant relative temperature jump, even with smaller particles. For these cases, there is no measurable variation with pressure, so the data are presented in tabular form (see Table 2). The uncertainty in the value of h is ±10–20%.

Binary beds have higher packing fraction and a larger number of contact points, so that one expects less contribution from the gas phase. This seems to be born out by the data. The He and N_2 data are nearly identical for a given particle mixture and do not depend on pressure. The wall conductance for the 0.1+4.3 mm bed is substantially lower than the 0.5+4.3 mm bed. This is consistent with the single-size thermal conductivity data (Figs. 3–5) which indicates that the powder has much lower conductivity than the other two sizes in the regime dominated by metal-to-metal contact (i.e., with N_2 or low pressure He). The lower conductivity may be explained by the different surface characteristics of the powder. The 100-micron gas-atomized powder has a very rough surface, irregular shape, and probably more oxide near the surface. The data also suggest that the binary wall conductance is dominated by the small size fraction.

6. Conclusion

Data have been accumulated for metallic packed beds to simulate a Be bed which could be used in solid breeder fusion reactor blankets. Data were presented for a range of He and N_2 gas pressures, for several single-size and binary beds of aluminum, and for a number of different porosities. The effective thermal conductivity of the packed beds shows substantial variation with gas pressure – in some cases as much as a factor of 4. The dependence on porosity has been experimentally determined.

In most cases the wall temperature jump is relatively small compared to the temperature difference across the bed. The relative effect is smallest in single-size beds with smaller particles. The variation of wall conductance with pressure is small or non-existent, suggesting that the wall region is dominated by conduction through the solid particle contact points, rather than gas in the Smolukovski zones.

Acknowledgements

This work was supported under US DOE contract #DE-FG03-86ER52123.

References

[1] A. R. Raffray, et al., "Thermal Control of Solid Breeder Blankets," proceedings of this symposium.

[2] M. A. Abdou, et al., "A Helium-Cooled Solid Breeder Concept for the Tritium-Producing Blanket of the International Thermonuclear Experimental Reactor," Fusion Tech. 15(2), Part 1 (1989) 166–182.

[3] Z. R. Gorbis, et al., "Thermal Resistance Gaps for Solid Breeder Blankets Using Packed Beds," Fusion Tech. 15 (1989) 695–698.

[4] M. S. Tillack, et al., "Experimental Study of the Effective Thermal Conductivity of a Packed Bed as a Temperature Control Mechanism for ITER Ceramic Breeder Blanket Designs," 13th Symposium on Fusion Engineering, Knoxville TN, October (1989).

[5] Philip R. Bevington, "Data Reduction and Error Analysis for the Physical Sciences," McGraw-Hill Book Company, New York (1969).

Table 1. Particle sizes and packing fractions obtained

Bed type	Particle sizes	Packing fraction range
gas-atomized powder	75–150 μm	57–59%
centrifugally-atomized shot	0.4–0.7 mm	60–64%
ball bearings	4.3 mm	62–65%
binary	4.3+0.5 mm	80–86%
binary	4.3+0.1 mm	83–87%

Table 2. Wall conductance for binary beds with He and N_2 fill gas

Particle sizes (mm)	Fill gas	Packing fraction (%)	h (W/m^2-K)
4.3+0.5	He	86.1	880
4.3+0.5	N_2	86.1	870
4.3+0.1	He	87.1	550
4.3+0.1	N_2	87.1	540

Figure 1. Particle bed test section

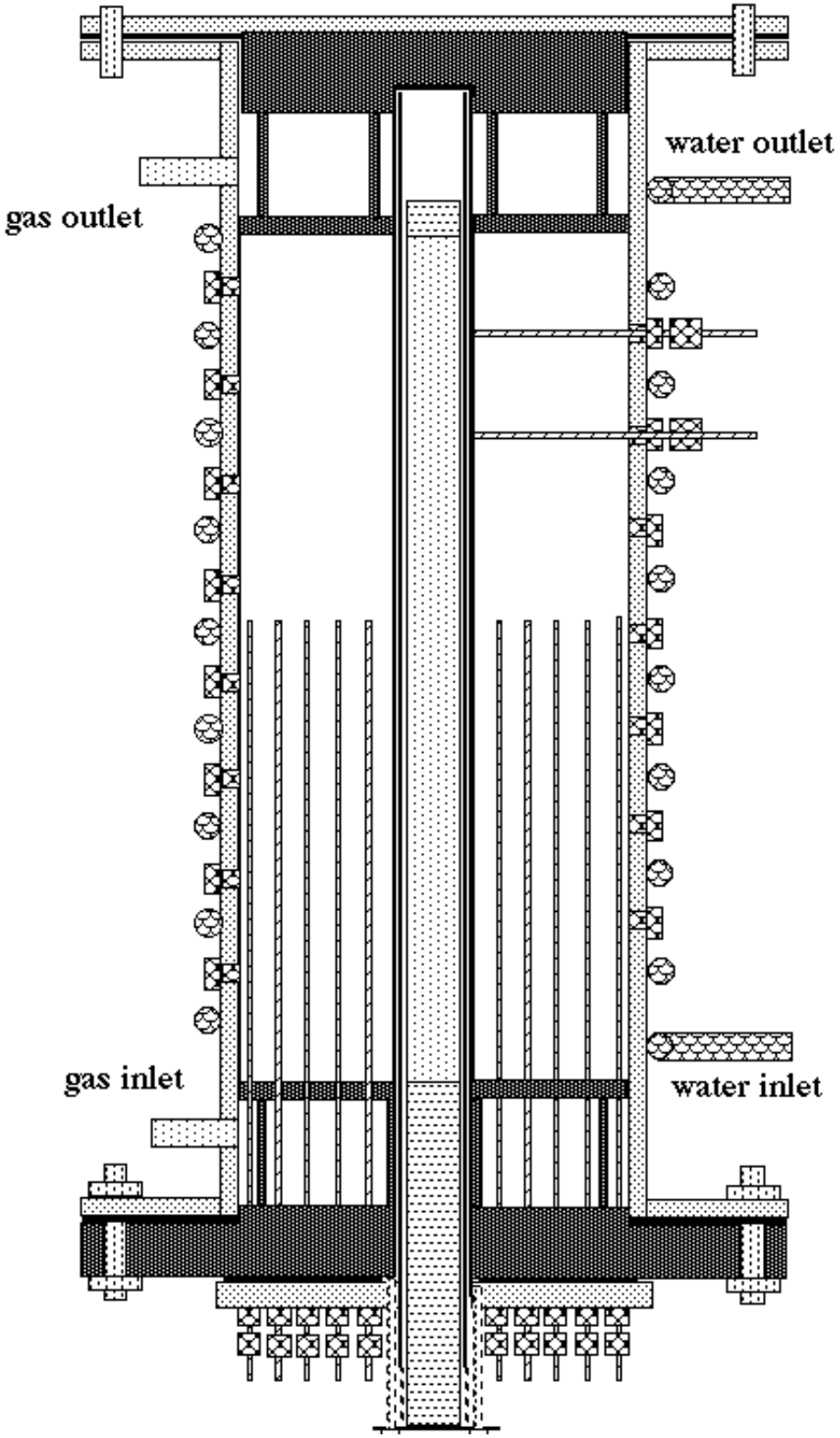

Figure 2. Gas flow circuit

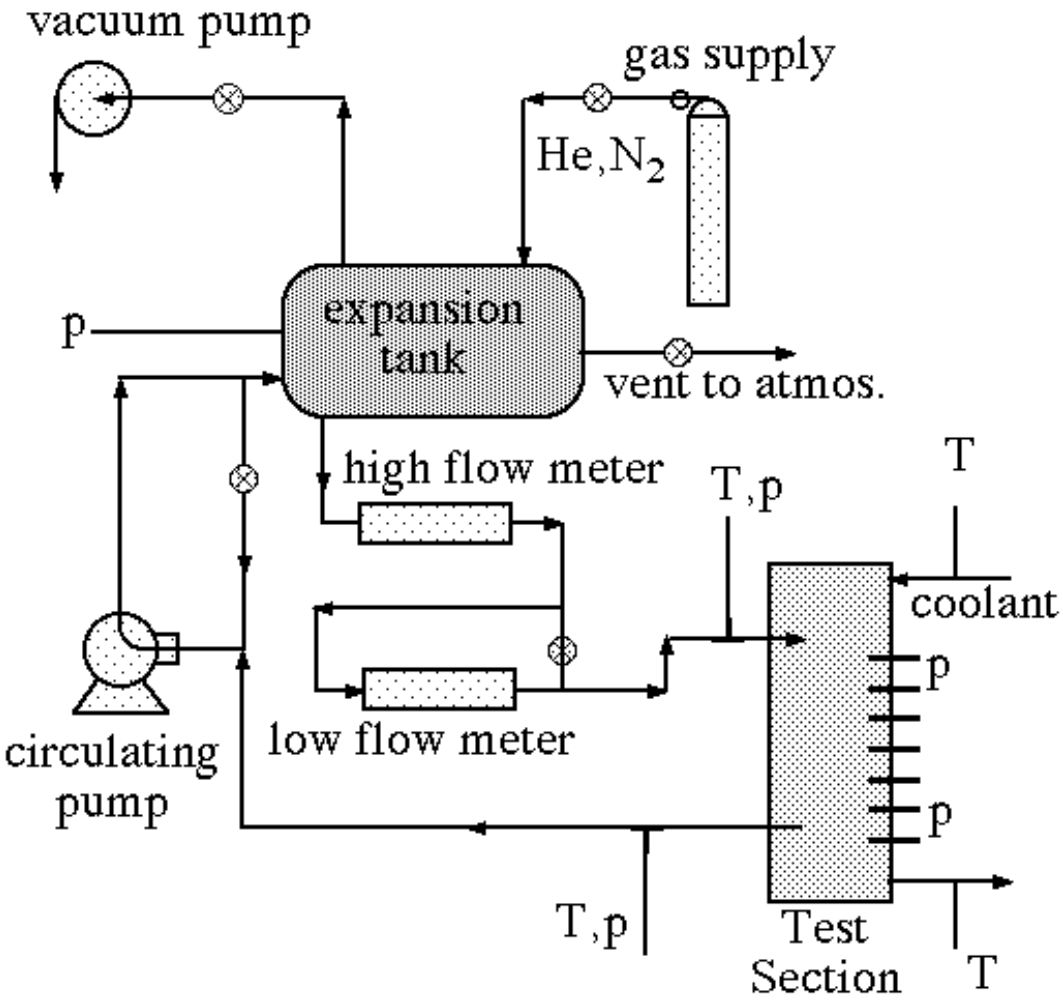

Figure 3. Thermal conductivity vs. gas pressure in 4.3-mm Al beds (with packing fractions 62.6 and 65%) with He and N_2 fill gas. Open circles denote previously reported data.

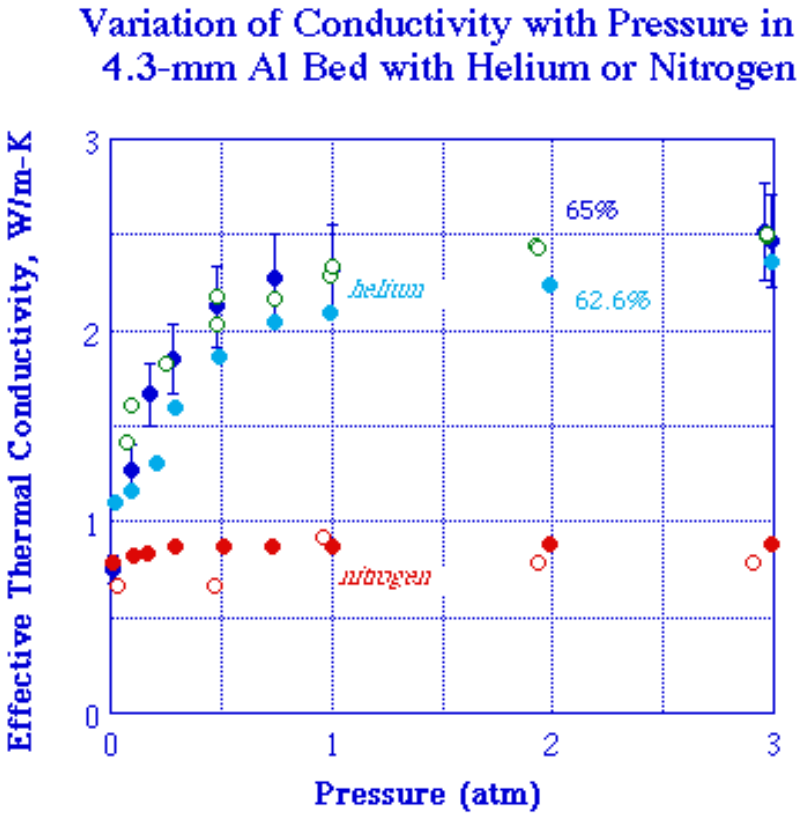

Figure 4. Thermal conductivity vs. gas pressure in 0.5-mm Al beds (with packing fractions 60.3 and 62.4%) with He and N_2 fill gas. Open circles denote He and closed circles denote N_2.

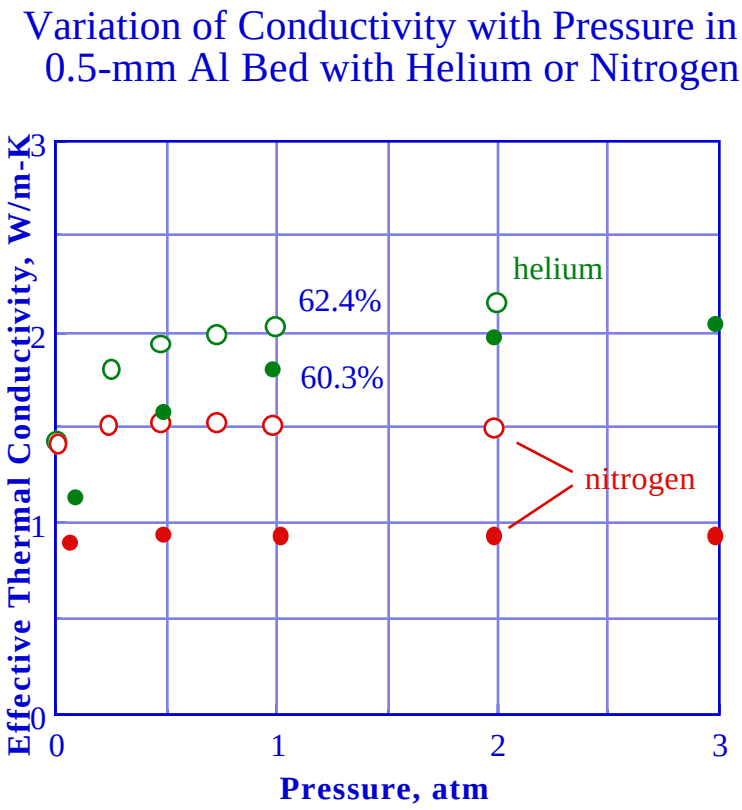

Figure 5. Thermal conductivity vs. gas pressure in 0.1-mm Al beds (with packing fractions 57.4 and 58.8%) with He and N_2 fill gas. Open circles denote previously reported data.

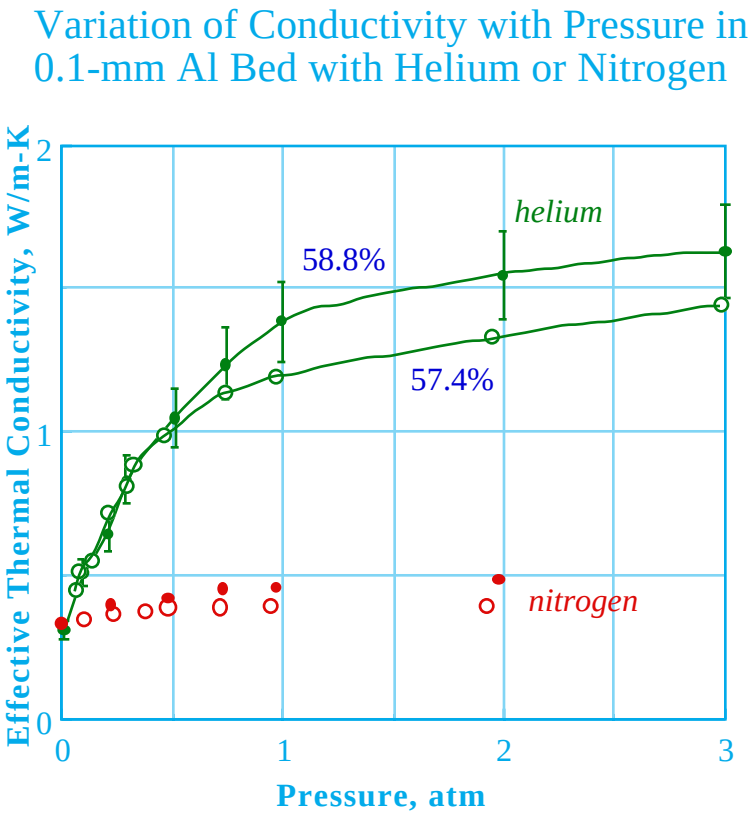

Figure 6. Thermal conductivity vs. gas pressure in 0.5+4.3-mm Al binary beds with He and N_2 gas and several packing fractions. Open circles denote He and closed circles denote N_2.

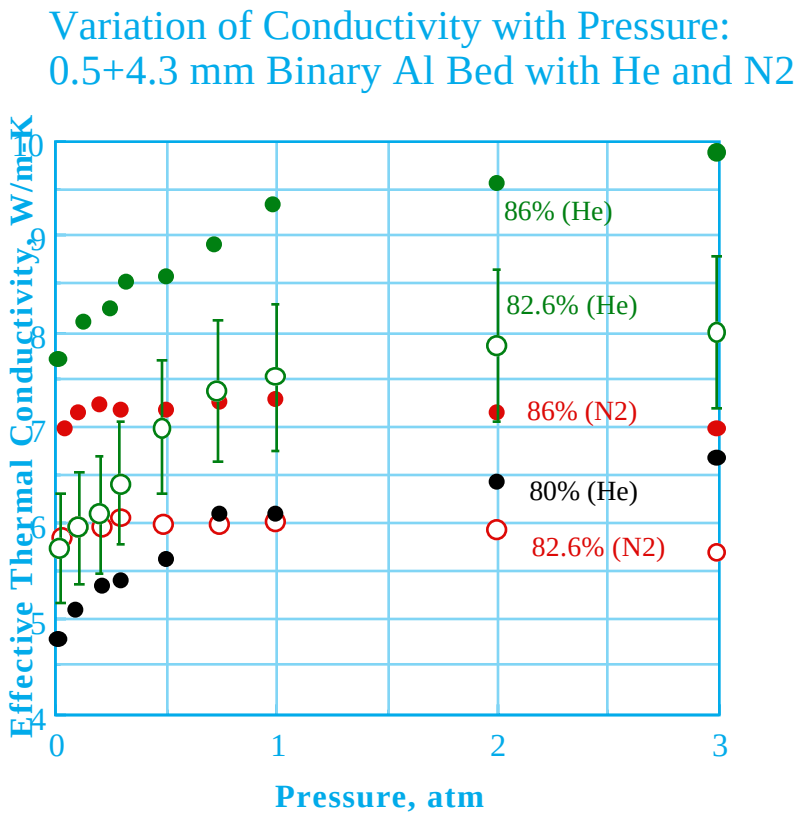

Figure 7. Thermal conductivity vs. gas pressure in 0.1+4.3-mm Al binary beds with He fill gas and several packing fractions.

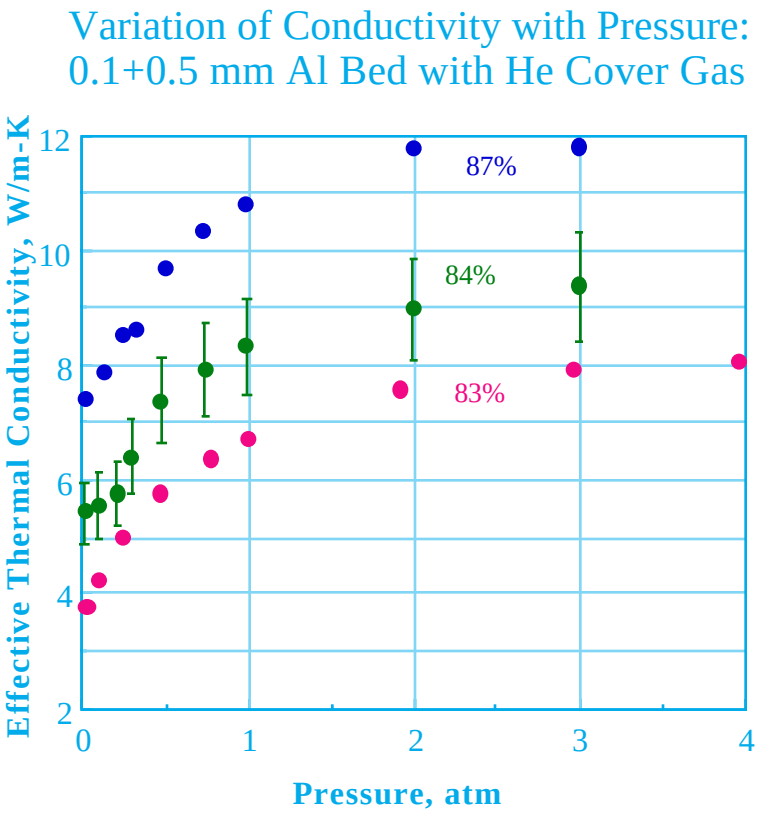

Figure 8. Wall conductance for 4.3-mm balls with He and N_2 fill gas.